

## LARGE-SYSTEM HYDRODYNAMIC LIMIT

WILLIAM G. HOOVER<sup>1</sup> AND HARALD A. POSCH<sup>2</sup>

<sup>1</sup> *Department of Applied Science, L-794 University of California  
at Davis and Lawrence Livermore National Laboratory  
Livermore, California USA 94551-7808*

<sup>2</sup> *Institute for Experimental Physics, Universität Wien, Boltzmannngasse 5  
A-1090 Vienna, Austria*

**ABSTRACT:** Parallel computers and fast work stations are helping to reveal ever-more-detailed, even unexpected, aspects of microscopic chaos and macroscopic instability in atomistic and continuum flows. Reproducing the chaos and the instabilities tests the integrators and the novel boundaries required by nonequilibrium simulations. Here, by adding appropriate boundary, constraint, and driving forces to the atomistic interparticle forces, we have simulated a wide range of homogeneous ergostatted two-dimensional shear flows with up to 264 196 particles. Our results demonstrate hydrodynamic stability, as well as freedom from long-time-tail divergence and turbulence, for Reynolds numbers as high as 50 000. This unexpected stability, despite large-scale fluctuations and microscopic chaos, makes it possible to define a two- or three-dimensional nonequilibrium "hydrodynamic limit" for shear flows analogous to the equilibrium "thermodynamic limit".

### I. INTRODUCTION

Parallel computers have made simulations with millions [1], or even billions [2], of degrees of freedom possible. In problems with rapidly-changing connectivity (automobile collisions are a good example [3]) the dynamic distribution of nodes among processors is a challenge. In the simpler problems of confined hydrodynamic flows, treated with particle methods, the distribution of the atoms, or the computational nodes, among cells, and the further distribution of these cells among processors, can be handled efficiently by describing the developing connectivity with "linked lists" [4] of cell occupants, with cells chosen large enough that only particles in neighboring cells can interact.

Simulations have recently become sufficiently detailed to characterize the general features of turbulent flows. Numerical simulations of macroscopic turbulence show that deviations from the predictions of Kolmogorov's simple dimensional analysis of the turbulent energy cascade [2], though real, are small. Frisch and Orszag [5] attribute the discrepancies to intermittent fractal structures in the turbulent flows. Because constitutive relations must be *assumed* from the beginning in the macroscopic continuum approach, microscopic atomistic flow simulations can provide more fundamental knowledge than can the macroscopic ones. Microscopic simulations *generate* the constitutive relations.

Mathematicians use the term “flow” to describe the time-dependent solution of differential deterministic equations of motion, either in a microscopic phase space, or in a macroscopic solution space. Quite generally, interesting hydrodynamic flows correspond to mathematical phase- or solution-space flows which are *Lyapunov unstable*. This means *exponential* growth, in time, of the separation of representative points tracing out neighboring trajectories, either in microscopic phase space or in macroscopic state space. Interesting hydrodynamic flows are typically *dissipative*, as well as Lyapunov unstable.

In geometric terms dissipation corresponds to state-space contraction. Imagine the time-development of all the trajectories initiated at a very large, but finite, set of similar initial conditions, with those initial points uniformly filling a phase-space or solution-space hypersphere. The governing flow equations are said to be “dissipative” if the time-dependent hypervolume spanned by the moving representative points contracts. In the atomistic case, the flow occurs in phase space, and the contraction reflects the extraction of heat from the system. Both microscopic and macroscopic dissipative flows contract and collapse onto a phase-space or state-space strange attractor with a dimension less than that of the embedding space.

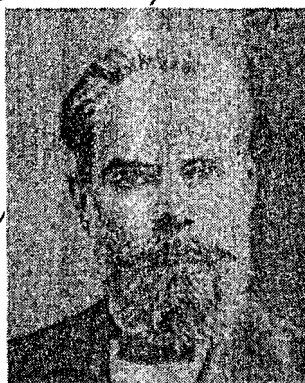
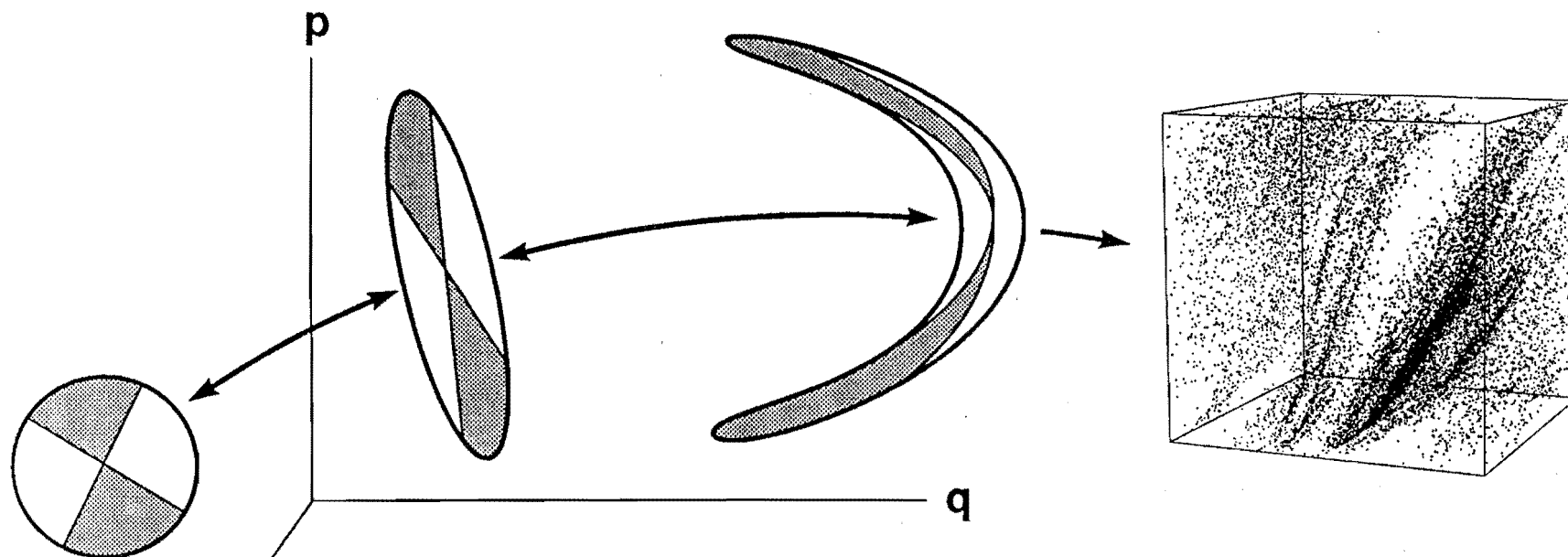
Equilibrium microscopic flows follow Liouville’s Theorem and do not collapse, but are nevertheless Lyapunov unstable. The spectrum of the time-averaged growth and decay rates of hypervolumes in state space or phase space is termed the *Lyapunov spectrum*. The largest Lyapunov exponent,  $\lambda_1$ , describes the rate at which two neighboring trajectories separate  $\propto \exp[\lambda_1 t]$ . In a bounded space, the exponentially-growing separation between neighboring trajectories must eventually stop. Eventually the separation between bounded trajectories requires a nonlinear description which corresponds to bending and folding motions seen in mixing cream with coffee or in kneading bread. The simplest mathematical caricature of such a folded structure is the “Smale Horseshoe” illustrated in the center of Figure 1.

The details of the infinitesimally-small-scale linear deformation, well below the finite scale associated with bending and folding, are described by the Lyapunov spectrum  $\{\lambda_i\}$ . The sum of the first two exponents gives the rate at which the area defined by *three* nearby trajectories, grows,  $\propto \exp[\lambda_1 t + \lambda_2 t]$ , and so on. For stationary dissipative systems, the sum of *all* the exponents,  $\Sigma \lambda_i$ , is universally negative. The sum gives the rate at which comoving phase volume collapses toward a dissipative strange attractor:

$$\frac{d \ln V_{\text{phase}}}{dt} \equiv \Sigma \lambda_i.$$

For microscopic atomistic systems this collapse is the manifestation of the macroscopic Second Law of Thermodynamics [6, 7].

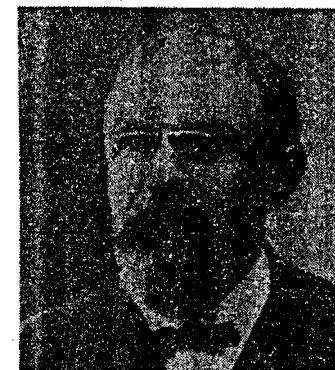
# GENERIC NONEQUILIBRIUM IRREVERSIBLE BEHAVIOR



LYAPUNOV



SMALE



POINCARÉ

Fig. 1. The initial exponential growth of phase-space hypervolumes, shown to the left of center, leads next to the formation of Smale horseshoes, and finally to collapse, onto a multifractal strange attractor. A typical "Poincaré" attractor cross-section is shown at the right.

Away from equilibrium, the exponential stretching, bending, and collapse are accompanied by a reduction in *dimensionality* of the phase-space distribution. The collapse eventually settles on a fractal object of the kind shown at the right in Figure 1. The spectra of Lyapunov exponents can also be obtained for continuum systems, and are likewise characterized by multifractal strange attractors in the corresponding macroscopic state space [8]. The importance of the fractal nature of the attractors is twofold. First, the dimensionality indicates the number of independent variables required for a detailed description of the nonequilibrium state. Second, and more speculatively, it seems likely that the relative probability of coexisting solution-space attractors, can be estimated by comparing the fractal dimensions of their hypervolumes, with the higher-dimensional objects being more probable than their lower-dimensional competitors.

The atomistic approach is limited to small time and space scales, microseconds and micrometers. How can we improve upon the limited efficiency of direct atomistic simulation? For gases, we can eliminate the need to treat the detailed particle-particle interactions, except statistically, by using Bird's stochastic method for solving the Boltzmann Equation. This gas-phase approach makes it possible to study far-from-equilibrium flows and instabilities with 10 to 100 times better resolution than molecular dynamics can achieve [9]. For condensed phases, we can increase the scale with *macroscopic* particles, rather than atoms, using smoothed-particle applied mechanics [10] to provide expanded time and space scales, as well as immunity from mesh-tangling. See Figure 2 for an illustration of Rayleigh-Bénard instability, a typical unstable hydrodynamic flow. Each of the smoothed particles shown in the Figure represents a localized, but smoothed out distribution of mass, with the mass distributed according to a smoothing or weighting function  $w(r)$ . With astronomically large masses and weighting-function ranges, this same particle method, "Smoothed-Particle Applied Mechanics", can even be applied to extraterrestrial astrophysical events, as in the successful recent modeling of the collisions of Shoemaker-Levy 9 comet fragments with Jupiter [11].

In a very special case, the smoothed-particle method displays an interesting isomorphism with pairwise-additive-force molecular dynamics, with the smoothed-particle trajectories identical to atomistic particle trajectories [12]. In this special case the smoothed-particle weighting function  $w(r)$  must be chosen to have the same shape as does the atomistic pair potential  $\phi(r)$ . "Hybrid methods" combining the weighting-function and potential-based approaches should make it possible to bridge the gap in spatial resolution which now separates microscopic and macroscopic simulations.

The rapidly-increasing speed and scale of fast computers has spawned new techniques and capabilities. These consequences of engineering advances can reverse the usual pattern of searching for techniques to solve particular problems. One can equally-well search for problems suited to the new techniques. Which of the many problems open to investigation are worth solving? Three answers to this question were

discussed at a stimulating Symposium on Computer Simulation at Røros, for which this manuscript was prepared:

(i) the coupling between heat and mass flows was studied by observing the concentration gradient developing in a system confined between two walls of unlike temperature [13];

(ii) the fluid-solid coexistence curve has been mapped out for the entire family of inverse power potentials,  $\phi(r) \propto r^{-n}$ , by varying the interparticle force law as the computer simulation proceeds. [14]

(iii) by using molecular dynamics to study the short-time diffusion of a slab of tagged particles the failure of the Maxwell-Cataneo approach to nonlinear irreversible thermodynamics has been documented [15].

Each of these three interesting studies combines old microscopic material models with a new type of simulation technique so as to answer interesting, previously unanswerable, questions.

An enduring general problem for both macroscopic and microscopic simulations is establishing credibility for the chosen numerical algorithms. We believe that the study and understanding of *instabilities* [16], both microscopic Lyapunov instabilities and macroscopic hydrodynamic ones, and analysis of the ability of numerical schemes to reproduce these instabilities faithfully, is the key to validating the schemes. In Sections II and III we describe simple integration algorithms as well as the special boundary conditions adapted to nonequilibrium simulations. In Section IV we describe the theoretical reasons for expecting macroscopic instabilities in two-dimensional shear flows. In striving to characterize this high-strain-rate instability of two-dimensional shear flows, we found instead, to our surprise, *stability*. We describe the shear-flow simulations and our numerical results in Section V. We point out there that the size-independence of the shear viscosity suggests the utility of a nonequilibrium "hydrodynamic limit" analogous to the well-known equilibrium "thermodynamic limit" of Gibbsian statistical mechanics.

## II. EQUILIBRIUM ALGORITHMS FOR MOLECULAR DYNAMICS

Even for microscopic atomistic systems, equilibrium is the simplest situation, with time-reversible and deterministic equations of motion. The simplest approximate integration scheme which retains the time-reversible character of the underlying differential equations is the remarkably-stable Störmer integrator [17, 18],

$$\left\{ \frac{[q_{t-dt} - 2q_t + q_{t+dt}]}{dt^2} = a_t \right\}.$$

A series expansion of  $q_t - dt$  in powers of  $dt$  shows that the local one-step coordinate error is of order  $dt^4$ , so that the accuracy of the coordinates  $\{q\}$  generated by this algorithm is locally third-order. Because *two* integrations with respect to time are required, the corresponding global error is second-order in  $dt$ . In practice this accuracy is degraded by Lyapunov instability, so that the local integration error acts as a “seed” with long-time trajectory errors proportional both to the seed and to  $\exp[\lambda_1 t]$ .

RAYLEIGH-BÉNARD PROBLEM  
IMAGE-PARTICLE BOUNDARY CONDITIONS  
OYEON KUM'S SPAM SIMULATION

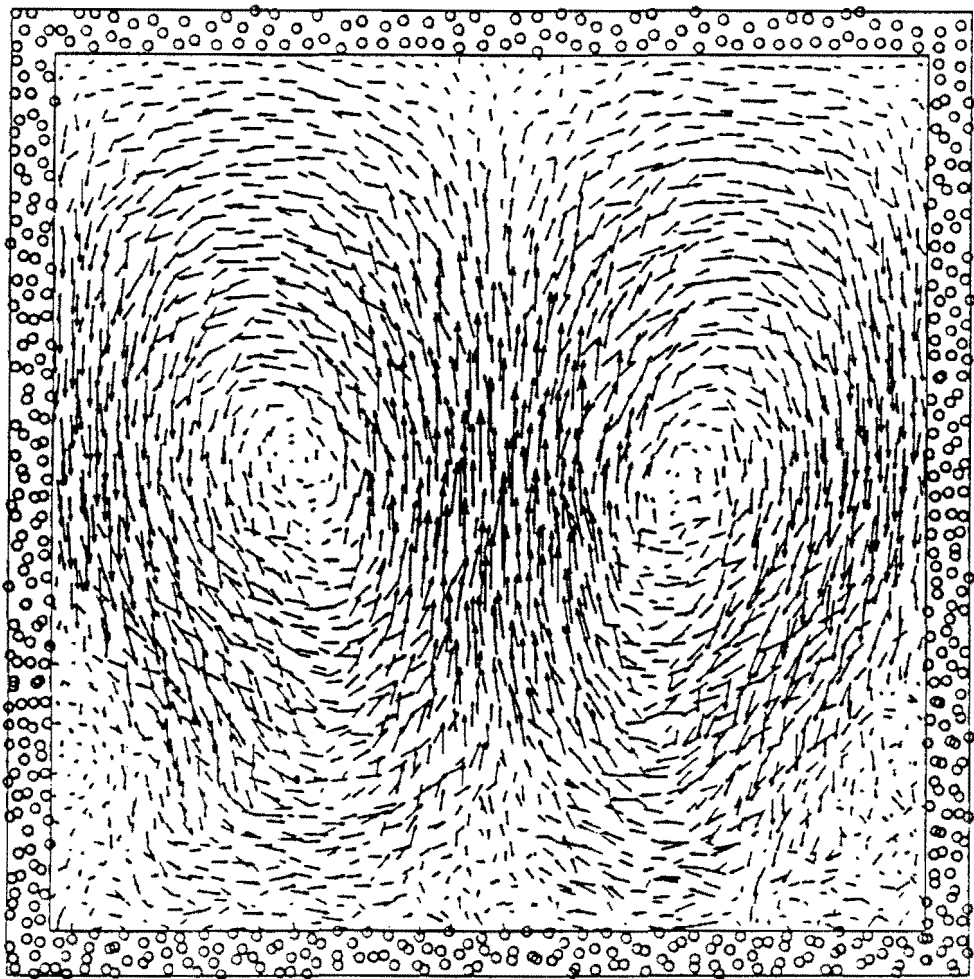


Fig. 2. Sample frame of a Smoothed-Particle Applied Mechanics simulation of the Rayleigh-Bénard instability problem using reflecting boundary conditions. The particles in the boundary strip are reflected images of those inside. The strip width is equal to the range of the smoothing function. The convective flow of heat is induced by a hot lower boundary, a cold upper boundary, and a strong vertical gravitational field.

Higher-order accuracy requires not just better integrators, but also more continuous derivatives of the accelerations. For example, the smooth repulsive potential,

$$\phi(r) = 100\epsilon[1 - (r/\sigma)^2]^4; \quad r < \sigma,$$

has a discontinuity in the fourth derivative,  $\phi''''$ . During the time step  $dt$ , with a corresponding coordinate displacement  $vdt$ , when the cubic force field is first entered, the averaged force is in error by an amount of order  $\phi''''(vdt)^3$ , leading to a local one-step coordinate error of order  $(\phi''''v^3/m)dt^5$ . This one-step error is no worse than those generated by the classic fourth-order Runge-Kutta integrator, or Milne's locally fifth-order, globally third-order, implicit scheme [19]:

$$\left\{ \frac{[q_{t-dt} - 2q_t + q_{t+dt}]}{dt^2} = \left( \frac{1}{12} \right) [a_{t-dt} + 10a_t + a_{t+dt}] \right\}.$$

In the work we describe here we use the classic fourth-order Runge-Kutta integrator because its treatment of velocities and constraints is more easily implemented.

Isolated systems obey Hamilton's or Schrödinger's time-reversible motion equations. Away from equilibrium, the simulation of stationary bounded nonequilibrium flows requires generalizing these mechanics so as to include special constraint and driving forces to play the roles of energy sources and sinks. It still is beneficial, even in this case, to continue to use deterministic and time-reversible equations of motion, and algorithms, to describe nonequilibrium problems. A new understanding of the link between reversible microscopic dynamics and irreversible macroscopic thermodynamics, which has a long history of puzzling physicists despite Boltzmann's H Theorem explanation, has come from analyzing the results of deterministic time-reversible nonequilibrium molecular dynamics [17]. The new deterministic approach provides the basis for a quantitative analysis, and understanding, of the symmetry breakings (always present in time, and often present in space) associated with nonequilibrium flows.

Deterministic forces, as opposed to stochastic ones, have another advantage in analyzing nonequilibrium flows. Determinism makes possible direct quantitative inter-comparisons of results among different investigators.

### III. BOUNDARIES, CONSTRAINTS, AND DRIVING FORCES

Away from equilibrium, energy sources and heat sinks must be provided. In the atomistic case, boundary values of stream velocity, energy, temperature, pressure tensor, and heat flux vector, can be fixed or controlled by Lagrange multipliers. The simplest example of such control is the Gaussian thermostat [20], which fixes the kinetic temperature of a specified set of degrees of freedom through a time-varying control parameter or "friction coefficient"  $\zeta$ :

$$\left\{ \dot{q} = \frac{p}{m}; \dot{p} = F - \zeta p \right\}; \zeta \equiv \frac{\sum F \cdot p}{\sum p^2}.$$

These motion equations satisfy, identically, the kinetic energy constraint:

$$\dot{K} \equiv \sum \left( \frac{p}{m} \right)_i \cdot \dot{p}_i \equiv \sum \left( \frac{p}{m} \right)_i \cdot F_i - \frac{\sum \left( \frac{p}{m} \right)_i \cdot p_i \sum F_j \cdot p_j}{\sum p_j^2} \equiv 0.$$

Note the *time-reversibility* of the motion equations for  $\{\dot{q}, \dot{p}\}$  as well as the constraint equation for  $\dot{K}$ . In a *time-reversed* solution  $p$ ,  $\zeta$ , and  $\dot{K}$  change sign, while  $q$ ,  $F$ , and  $K$  do not.

The Runge-Kutta integrators, which integrate first-order differential equations are easily applied to constrained systems. Some other integrators, such as Störmer's, are readily generalized to these cases<sup>17</sup>. There is no apparent way to adapt or extend "symplectic integrators", such as the implicit Runge-Kutta integrator described by Janei at the Røros meeting [21], to the nonequilibrium case. This lack suggests a promising research area.

In order to describe nonequilibrium interactions between atomistic systems and their surroundings, Ashurst [22] invented time-reversible "fluid walls". These boundaries minimize the spatial ordering of flows confined by external double-walled boundary regions. The total momentum and kinetic energy of the boundary particles confined within any fluid-wall region are constrained to specified boundary values imposing velocity and temperature constraints on the enclosed system.

In modeling the continuum case, with *smoothed particle applied mechanics*, [often referred to in the literature as "smoothed-particle hydrodynamics", or SPH] it is convenient to use related, but distinct, *reflecting* boundary conditions [23]. See Figure 2. Here, any particles within the range of the smoothing function (analogous to a pair potential), can interact with external *mirror-image* particles. The smoothed-particle equations make it possible to assign boundary velocities and temperatures to all the exterior "image particles" which differ from those of the interior particles which they image. Tests of all these ideas, and their variations, can be based on the ability of the corresponding simulations to reproduce known hydrodynamic instabilities [16], such as the Kelvin-Helmholtz, Rayleigh-Bénard [24], Rayleigh-Taylor, and Richtmyer-Meshkov instabilities. The simplest of these is the constant-volume Rayleigh-Bénard instability of Figure 2, in which buoyant convection currents are driven by thermal expansion. The rest involve the unstable and unbounded deformations of two relatively-moving materials sharing an unstable common boundary. The relative motion can be either parallel or perpendicular to the boundary and is initially exponentially

unstable. In the Richtmyer-Meshkov case the acceleration of a heavy material into a lighter one is provided by a shockwave, rather than by the gravity which drives Rayleigh-Bénard and Rayleigh-Taylor instabilities.

#### IV. THEORY OF TWO-DIMENSIONAL SHEAR FLOWS

To take advantage of recent advances in computer power, we chose to investigate the long-standing claim that two-dimensional transport coefficients diverge [25, 26]. The basis of this divergence must lie in the relative importance of fluctuations, in two dimensions. Because these fluctuations are the same order of magnitude as surface effects, of order  $N^{1/2}$  in both cases, it is plausible that the transport coefficients can diverge logarithmically with system size, just as does the rms displacement in a two-dimensional crystal [27].

Wainwright, Alder, and Gass [28] summarize the theoretical arguments leading to a logarithmic divergence of the Green-Kubo expression for the shear viscosity:

$$\begin{aligned}\eta(t \rightarrow \infty) &= \left( \frac{V}{kT} \right) \int_0^{t \rightarrow \infty} \langle P_{xy}(0) P_{xy}(t') \rangle_{\text{EQUILIBRIUM}} dt' \approx \\ &\approx \left( \frac{mV}{4\pi\eta kT} \right) \langle P_{xy}^2 \rangle \int_0^{t \rightarrow \infty} d \ln t' \approx \left( \frac{mV}{8\pi\eta kT} \right) \langle P_{xy}^2 \rangle \ln N.\end{aligned}$$

Their calculations for the coefficient of the  $(1/t)$  decay follow from hydrodynamic estimates of the long-time decay of shear stresses initiated by a small moving fluid volume element, and involve a relatively-complex combination of thermodynamic and transport properties. One could equally plausibly consider the decay of shear stresses initiated by plane transverse velocity waves. Because stress is proportional to the velocity gradient, the stress-stress correlation would vary as the square of the wave-vector, eliminating the  $1/t$  divergence.

If the hydrodynamic  $1/t$  decay is accepted, it seems reasonable to choose the sound-traversal time, proportional to  $N^{1/2}$ , as an upper limit on the integrated stress correlations. Thus, for long times, this approach implies a viscosity diverging as  $\ln t$ , or equivalently,  $\ln N$ . The possibility of understanding this intriguing paradox, that a patently finite ratio of stress to strain rate diverges, by using the increased computer power available today, led us to reinvestigate the problem of two-dimensional viscosities. Our earlier investigations [27, 29] had been inconclusive.

#### V. SIMULATION OF TWO-DIMENSIONAL SHEAR FLOWS

To reduce numerical errors, we use the classic fourth-order Runge-Kutta integration scheme, applied to the "Slod" equations of motion [30]:

$$\left\{ \dot{x} = \left( \frac{p_x}{m} \right) + \dot{\epsilon} y; \dot{y} = \left( \frac{p_y}{m} \right); \dot{p}_x = F_x - \dot{\epsilon} p_y - \zeta p_x; \dot{p}_y = F_y - \zeta p_y \right\};$$

$$\zeta \equiv \frac{-\dot{\epsilon} P_{xy} V}{2K}; K \equiv \sum \left( \frac{p^2}{2m} \right); P_{xy} V \equiv \sum \left( \frac{p_x p_y}{m} \right) - \sum \left( \frac{x_{ij} y_{ij} \phi_{ij}}{r_{ij}} \right),$$

the *kinetic* part of the pressure-tensor component  $P_{xy}$  includes a sum over all particles. The *potential* contribution is a sum over all  $N(N-1)/2$  distinct  $[i < j]$  pairs. The “momenta”  $\{p\}$  measure velocity relative to the mean flow,  $\langle v \rangle = y$ . The friction coefficient  $\zeta$  is chosen so as to maintain the internal energy,  $\epsilon + \Phi$ , constant in time. The forces have three continuous derivatives, as discussed

The “Lees-Edwards” boundary conditions [31] (developed also, independently, by Ashurst during his thesis work [22] at the Department of Applied Science in London) are consistent with a spatially-periodic shear. By using shearing periodic boundaries, we completely avoid the need for physical boundaries confining the fluid. In the simple two-particle version of the periodic model see Reference [32]. We measure the two-dimensional coefficient of shear viscosity  $\eta$  directly from the time-averaged shear stress:

$$\eta \equiv \frac{-\langle P_{xy} \rangle}{\dot{\epsilon}}.$$

Note that there is no connection between the potential energy parameter  $\epsilon$  and the strain rate  $\dot{\epsilon}$ ]

We have accumulated usable viscosity data over a relatively large range in  $N$ ,  $7 \leq 264, 196$ , covering more than three orders of magnitude. The data are detailed in the Tables. In Figure 3 we display these viscosities for two different strain rates, in the range of linear irreversible thermodynamics, and with the estimated standard deviations indicated, as a function of  $N^{-1/2}$ . We do not plot the data on a logarithmic scale because the expected theoretical slope is much too large to be consistent with our viscosity data. In all cases we study the moderately-dense-fluid state with total energy per particle equal to  $\epsilon$  and volume per particle equal to  $\sigma^2$ . Our data show a significant viscosity increase whatsoever for values of  $N$  larger than 2048. If, as suggested by Figure 3, the accurate number dependence is proportional to  $N^{-1/2}$ , then the largest-system results only deviate from the limiting viscosity by the statistical uncertainty of the data, about one part in 400. In Figure 4 we show the largest Lyapunov exponent,  $\lambda_{\max} \equiv \lambda_1$ , for the same simulations. That Figure suggests too, somewhat more strongly than does Figure 3, a size dependence varying as  $N^{-1/2}$ .

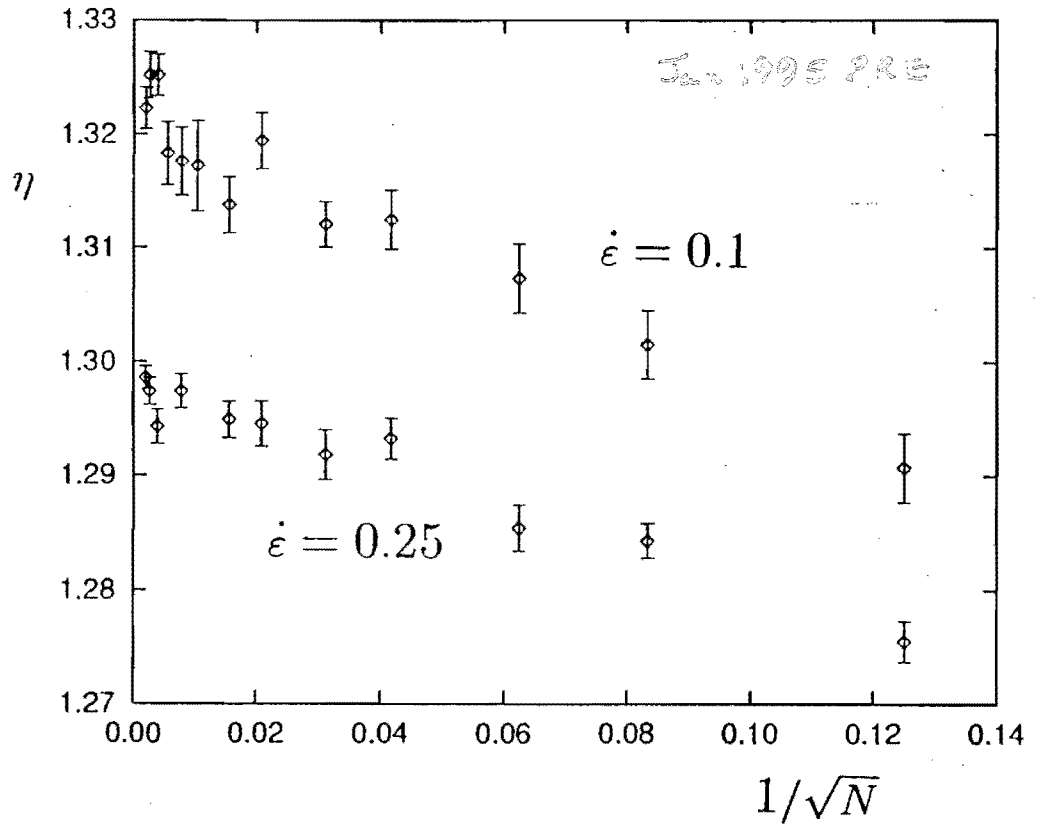


Fig. 3. Steady isoenergetic shear viscosities for  $N$  two-dimensional particles interacting with the potential  $100\epsilon[1 - (r/\sigma)^2]^4$ . The internal energy is equal to  $N\epsilon$ . Error bars indicate estimated standard deviations. The number of particles ranges from 64 ( $\ln N = 4.16$ ;  $N^{-1/2} = 0.125$ ) to 264,196 ( $\ln N = 12.48$ ;  $N^{-1/2} = 0.00195$ ). There is no significant change in the viscosity for  $N \geq 2048$ . Numerical values of the reduced viscosity coefficient have been plotted for two reduced strain rates where the potential parameters  $\epsilon$  and  $\sigma$ , as well as the particle mass  $m$  have all been set equal to unity.

As this work was being completed, Brad Holian kindly sent us a preprint [33] drawing similar conclusions, but based on rather different simulations of considerably smaller-scale two-dimensional viscous flows. We are not aware of any work establishing the divergence of the viscosity for any two-dimensional fluids. A careful lattice-gas study [34] of shear viscosity, with a sinusoidal velocity field, does provide good agreement with the predictions of mode-coupling theory – that is, the logarithmic divergence of viscosity with increasing system size. These simulations are quite different from ours. It is not at all clear how to introduce homogeneous shear into a lattice gas or into the mode-coupling theory.

We conclude, for the hydrodynamic state and strain rates studied here, that the hydrodynamic-limit shear viscosity is well defined, in two space dimensions, when a global constraint of constant energy is used to stabilize the nonequilibrium hydrodynamic state. Neither  $N$ -dependence nor hydrodynamic instabilities are observed, at Reynolds numbers as high as 50 000.

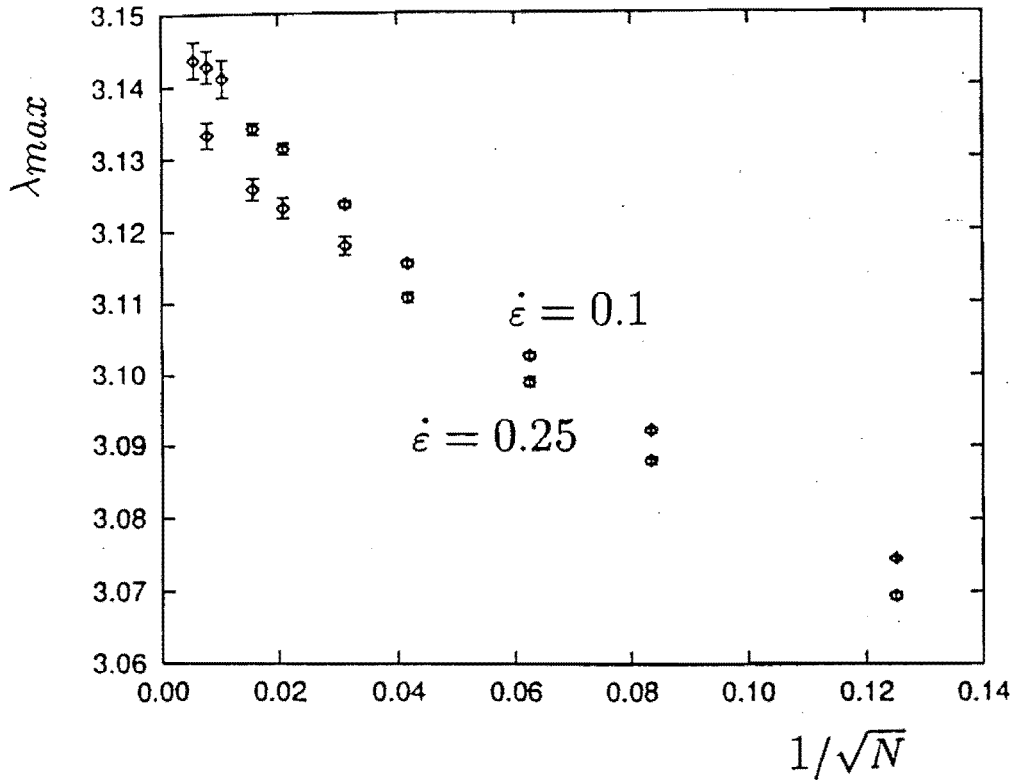


Fig. 4. Size-dependence of the maximum Lyapunov exponent for shear flows with  $N$  two-dimensional particles interacting with the potential  $100\epsilon[1 - (r/\sigma)^2]^4$ . The data cover the same simulations described in the Tables and in Fig. 3 and the units have been reduced in the same way.

Table I. Potential energy, shear viscosities, largest Lyapunov exponent, and shear-stress fluctuations for square periodic two-dimensional systems of  $N$  unit mass particles at unit density. The pair potential is  $100(1 - r^2)^4$ . The steady shear strain rate  $du_x/dy$  for all of these plane Couette flows is 0.10 and the total energy per particle,  $E/N \equiv [\Phi + K]/N$  is 1.000 in each case. The mean-squared fluctuation in the shear stress,  $\langle \Delta P_{xy}^2 \rangle$ , is expected to vary as  $1/N$ . The maximum shear for each run is indicated, where unit shear requires 2000 time steps of 0.005 each.

$N$	$\Phi/N$	$\lambda_1$	$\eta$	$\langle -P_{xy} \rangle$	$\langle N\Delta P_{xy}^2 \rangle$	$\epsilon_{\max}$
64	0.3052	3.074	1.291	0.129	8.52	40000
144	0.3042	3.092	1.302	0.130	8.47	18000
256	0.3039	3.103	1.307	0.131	8.44	11000
576	0.3036	3.116	1.312	0.131	8.43	6000
1024	0.3035	3.124	1.312	0.131	8.45	6000
2304	0.3034	3.131	1.319	0.132	8.44	2000
4096	0.3034	3.134	1.314	0.131	8.43	1000
9216	0.3034	3.141	1.317	0.132	8.32	200
16384	0.3033	3.143	1.318	0.132	8.42	160
32400	0.3033	3.144	1.319	0.132	8.55	110
65536	0.3033	—	1.325	0.132	8.49	140
146689	0.3033	—	1.325	0.132	8.51	50
*264196	0.3033	—	1.322	0.132	8.61	30

\* This number,  $514 \times 514$ , rather than  $512 \times 512$ , was used to improve the computational efficiency of the simulation.

Table II. Potential energy, shear viscosities, largest Lyapunov exponent, and shear-stress fluctuations for square periodic two-dimensional systems of  $N$  unit mass particles at unit density. The pair potential is  $100(1 - r^2)^4$ . The steady shear strain rate  $du_x/dy$  for all of these plane Couette flows is 0.25 and the total energy per particle,  $E/N \equiv [\Phi + K]/N$  is 1.000 in each case. The mean-squared fluctuation in the shear stress,  $\langle \Delta P_{xy}^2 \rangle$ , is expected to vary as  $1/N$ . The maximum shear for each run is indicated, where unit shear requires 800 time steps of 0.005 each.

$N$	$\Phi/N$	$\lambda_1$	$\eta$	$\langle -P_{xy} \rangle$	$\langle N\Delta P_{xy}^2 \rangle$	$\epsilon_{\max}$
64	0.3073	3.069	1.276	0.319	8.65	50000
144	0.3064	3.088	1.284	0.321	8.61	30000
256	0.3062	3.099	1.285	0.321	8.58	10000
576	0.3060	3.111	1.293	0.323	8.57	6200
1024	0.3059	3.118	1.292	0.323	8.61	4000
2304	0.3058	3.123	1.295	0.324	8.56	1200
4096	0.3058	3.126	1.295	0.324	8.52	1000
16384	0.3058	3.133	1.297	0.324	8.64	530
65536	0.3058	—	1.296	0.324	8.53	250
146689	0.3058	—	1.297	0.324	8.52	70
264196	0.3058	—	1.299	0.325	8.26	50

How can these high-Reynolds-number flows be stable? Microscopic Lyapunov instability, which would normally seed unstable, exponentially-growing vortical motions, is here controlled by the ergostat, which promotes exchange and damping of mode energies in such a way as to prevent the instability.

Heat flow can also be stimulated in nonequilibrium simulations, in a variety of ways. Control variables can be used to regulate the kinetic temperature, the energy, the stress, or the enthalpy, while a driving field maintains a variable, or stationary, heat current. It appears that homogeneous heat flow is more difficult to stabilize than shear flow. Several authors found that the Evans-Gillan algorithm for heat flow (which accelerates particles according to their energy and stress-tensor contributions at constant kinetic temperature) produces spatially-inhomogeneous unstable flows in two dimensions, evidently even for arbitrarily small values of the driving field [35-38]. This same instability might appear also in three dimensions. There is no published comprehensive intercomparison of the many similar distinct approaches to homogeneous heat flow. It is an excellent research topic for large-scale computation.

Because shear flow is successfully stabilized against instability by thermostating relative to the local mean velocity it seemed plausible that heat flow could be similarly stabilized, by thermostating [39]. We have tried many of these approaches ourselves, following Evans' work, and have so far always found instabilities similar to those which plagued Evans' original algorithm [38]. Using higher-order frictional force, proportional to  $p^3$ , reduces, but does not eliminate, the trend to instability [39]. We were unable to find a stable homogeneous heat-flow algorithm in two dimensions, and har-

bor the suspicion that three-dimensional systems can display a similar instability. But because, stable or not, this heat flow occurs without a temperature gradient, the conductivity simulations retain an artificial character.

As we emphasized recently [29], there is numerical evidence that our periodic boundary condition is much less intrusive than is a rigid one. It is therefore very desirable that quantitative transport theories be developed to take into account global boundary conditions of the type used here. As a consequence of this work, it seems apparent that a well-defined hydrodynamic limit for shear flows, analogous to the thermodynamic limit for equilibrium systems, can be defined as the large-system limit, at fixed density, energy, and strain rate, so that the list of state variables needs to be increased by only one in generalizing the concept of "state" away from equilibrium, to include shear. Of course there is a nonlinear variation of temperature and stress with strain rate too, so that the nonequilibrium constitutive relation is more complicated. But the existence of the large-system hydrodynamic limit dominates the influence of surface, wavelength, and frequency effects.

## VI. DISCUSSION

The present work demonstrates once again the power of simulation to provide surprises as a consequence of detailed results. The well-behaved nature of two-dimensional shear flows is a fortunate circumstance for simulation. Were the flows *not* well-behaved, the use of two-dimensional simulations to describe three-dimensional problems would be called into question. A potentially interesting area for investigation is the comparison of two- and three-dimensional simulations of otherwise identical hydrodynamic instabilities.

Because gains of at least two orders of magnitude in computer speed can be expected within the next decade, this is the moment to identify and resolve those nonequilibrium problems worthy of investigation using the new large-system tools.

**Acknowledgment:** Computations at the University of Vienna were supported by the University Computer Center and by the Austrian Fonds zur Förderung der Wissenschaftlichen Forschung Grant P9677. This work was performed, in part, under the auspices of the United States Department of Energy at the Lawrence Livermore National Laboratory under Contract W-7405-Eng-48. This work was presented at the Eighth Nordic Symposium on Computer Simulations (17 June 1994, Røros, Norway). Brad Holian, Oyeon Kum, Doug Miller, and Jim Viecelli furnished helpful advice and information. Asbjørn Hordvik and Kris Wojciechowski were responsible for its submission to Molecular Physics Reports in January of 1995.

(Received 5 January 1995)

## References

- [1] See the covers of the March-April 1992 and July-August 1993 issues of *Computers in Physics*.
- [2] E. S. Oran and J. P. Boris, *Computing Turbulent Shear Flows – A Convenient Conspiracy*, *Computers in Physics* 7, 523 (1993).

- [3] J. F. Chedmail, P. A. DuBois, A. K. Pickett, *Numerical Techniques, Experimental Validation, and Industrial Applications of Structural Impact and Crashworthiness Analysis with Supercomputers for the Automotive Industries*, in *Proceedings of the International Conference on Supercomputer Applications in the Automobile Industry*, C. Marino, Editor (Cray Research, Inc., Minneapolis, 1986).
- [4] R. W. Hockney and J. W. Eastwood, *Computer Simulations Using Particles* (Hilger, Bristol, 1988).
- [5] U. Frisch and S. A. Orszag, *Turbulence: Challenges for Theory and Experiment*, *Physics Today*, January 1990, 24.
- [6] W. G. Hoover, H. A. Posch, B. L. Holian, M. J. Gillan, M. Mareschal, C. Massobrio, *Dissipative Irreversibility from Nosé's Reversible Mechanics*, *Molecular Simulation* **1**, 79 (1987).
- [7] B. L. Holian, W. G. Hoover, H. A. Posch, *Resolution of Loschmidt's Paradox: The Origin of Irreversible Behavior in Reversible Atomistic Dynamics*, *Physical Review Letters* **59**, 10 (1987).
- [8] See the discussion of the work of Grappin and Leorat; their data are plotted for comparison with microscopic spectra in H. A. Posch and W. G. Hoover, *Equilibrium and Nonequilibrium Lyapunov Spectra for Dense Fluids and Solids*, *Physical Review A* **39**, 2175 (1989).
- [9] G. A. Bird, *The Direct Simulation Monte Carlo Method: Current Status and Perspectives*, in *Microscopic Simulations of Complex Flows*, M. Mareschal, editor (Plenum, New York, 1990).
- [10] J. J. Monaghan, *Smoothed Particle Hydrodynamics*, *Annual Review of Astronomy and Astrophysics* **30**, 543 (1992).
- [11] See two papers by N. M. Hoffman, R. F. Stellingwerf, and C. A. Wingate, *SPH Calculations of Comet Shoemaker-Levy 9/Jupiter Impact*, *Bulletin of the American Astronomical Society* **26**, 879, 880 (1994).
- [12] O. Kum and W. G. Hoover, *Time-Reversible Continuum Mechanics*, *Journal of Statistical Physics* **76**, 1075 (1994).
- [13] J. M. Kincaid, X. Li, and B. Hafskjold, *Nonequilibrium Molecular Dynamics Calculation of the Thermal Diffusion Factor*, *Fluid Phase Equilibria* **76**, 113 (1992).
- [14] A. D. J. Haymet, *Liquid/Solid Phase Transitions*, Invited Talk, 8th Nordic Symposium on Computer Simulation of Liquids and Solids (15-17 June 1994, Røros, Norway). See R. Agrawal and D. A. Kofke, *Thermodynamic and Structural Properties of Model Systems at Solid-Fluid Coexistence*, *Molecular Physics* **85**, 23 (1995).
- [15] J. M. Kincaid, *Studies of Heat and Mass Transfer Using Nonequilibrium Molecular Dynamics*, Invited Talk, 8th Nordic Symposium on Computer Simulation of Liquids and Solids (15-17 June 1994, Røros, Norway).
- [16] S. Chandrasekhar, *Hydrodynamic and Hydromagnetic Stability* (Oxford, Clarendon, 1961).
- [17] W. G. Hoover, *Computational Statistical Mechanics* (Elsevier, Amsterdam, 1991).
- [18] D. Levesque and L. Verlet, *Molecular Dynamics and Time Reversibility*, *Journal of Statistical Physics* **72**, 519 (1993).
- [19] W. E. Milne, *Numerical Calculus* (Princeton University Press, New Jersey, 1949).
- [20] W. G. Hoover, A. J. C. Ladd, B. Moran, *High-Strain-Rate Plastic Flow Studied via Nonequilibrium Molecular Dynamics*, *Physical Review Letters* **48**, 1818 (1982).
- [21] D. Janei and B. Orel, *Implicit Runge-Kutta Method for Molecular Dynamics Integration*, *Journal of Chemical Information and Computer Science* **33**, 252 (1993).
- [22] W. T. Ashurst, *Dense Fluid Shear Viscosity and Thermal Conductivity via*

- Nonequilibrium Molecular Dynamics*, Ph. D. Dissertation (University of California at Davis/Livermore, 1974).
- [23] O. Kum, *Nonequilibrium Flows with Smooth Particle Applied Mechanics*, Ph. D. Dissertation (University of California at Davis/Livermore, 1995).
- [24] D. C. Rapaport, *Unpredictable Convection in a Small Box: Molecular Dynamics Experiments*, *Physical Review A* **46**, 1971 (1992) and *Molecular Dynamics Study of Rayleigh-Bénard Convection*, *Physical Review Letters* **60**, 2480, 1988.
- [25] M. H. Ernst, E. H. Hauge, J. M. J. van Leeuwen, *Asymptotic Time Behavior of Correlation Functions*, *Physical Review Letters* **25**, 1254 (1970).
- [26] See the discussions given by J. R. Dorfman and W. W. Wood in *The Boltzmann Equation*, E. G. D. Cohen and W. Thirring, editors (Springer-Verlag, Wien, 1973), the Proceedings of an international symposium held in Vienna in September of 1972.
- [27] W. G. Hoover, W. T. Ashurst, R. J. Olness, *Two-Dimensional Computer Studies of Crystal Stability and Fluid Viscosity*, *Journal of Chemical Physics* **60**, 4043 (1974).
- [28] T. E. Wainwright, B. J. Alder, D. M. Gass, *Decay of Time Correlations in Two Dimensions*, *Physical Review A* **4**, 233 (1971).
- [29] W. G. Hoover and H. A. Posch, *Second-Law Irreversibility and Phase-Space Dimensionality Loss from Time-Reversible Nonequilibrium Steady-State Lyapunov Spectra*, *Physical Review E* **49**, 1913 (1994).
- [30] D. J. Evans and G. P. Morriss, *Nonequilibrium Liquids* (Academic, New York, 1990).
- [31] A. W. Lees and S. F. Edwards, *The Computer Study of Transport Processes under Extreme Conditions*, *Journal of Physics C* **5**, 1921 (1972).
- [32] A. J. C. Ladd and W. G. Hoover, *Lorentz Gas Shear Viscosity via Nonequilibrium Molecular Dynamics and Boltzmann's Equation*, *Journal of Statistical Physics* **38**, 973 (1985).
- [33] D. Gravina, G. Ciccotti, B. L. Holian, *Linear and Nonlinear Viscous Flow in Two-Dimensional Fluids* (preprint, 1994).
- [34] L. P. Kadanoff, G. R. McNamara, G. Zanetti, *From Automata to Fluid Flow: Comparisons of Simulation and Theory*, *Physical Review A* **40**, 4527 (1989).
- [35] D. J. Evans and H. J. M. Hanley, *Heat Induced Instability in a Model Liquid*, *Molecular Physics* **68**, 97 (1989).
- [36] M. Mareschal and A. Amella, *Thermal Conductivity in a One-Dimensional Lennard-Jones Chain by Molecular Dynamics*, *Physical Review A* **37**, 2189 (1988).
- [37] W. Loose, *Thermal Transport in Gases via Homogeneous Nonequilibrium Molecular Dynamics*, *Physical Review A* **40**, 2625 (1989).
- [38] D. P. Hansen and D. J. Evans, *Generalized Heat Flow Algorithm*, *Molecular Physics* **81**, 767 (1994).
- [39] W. G. Hoover and H. A. Posch, *Shear Viscosity via Global Control of Spatio-Temporal Chaos in Two-Dimensional Isoenergetic Dense Fluids*, *Physical Review E* **51**, 273 (1995); see also H. A. Posch, W. G. Hoover, O. Kum, *Steady-State Shear Flows via Nonequilibrium Molecular Dynamics and Smooth Particle Applied Mechanics*, *Physical Review E* (August, 1995).